J MATER SCI **41** (2006) 719–725

The origin of asterism in almandine-pyrope garnets from Idaho

MAXIME J-F GUINEL, M. GRANT NORTON
Washington State University, School of Mechanical and Materials Engineering, PO Box 642920, Pullman, WA 99164-2920, USA

We have shown that the asterism in garnets emanating from Emerald Creek, Latah County, Idaho, is due to the precipitation of acicular crystals in the garnet crystal host. These inclusions have been identified, using electron microscopy, as tetragonal rutile, the stable phase of TiO_2. One set of rutile (r) needles was found to have the following crystallographic relationship with its garnet (g) host: $[011]_g // [0\bar{1}0]_r$, $(02\bar{2})_g // (100)_r$, $(\bar{4}00)_g // (001)_r$. From meticulous examinations of the asteriated garnets and the angular relationships between the rutile inclusions and the garnet matrix it was possible to determine the orientations of the other sets of needles for both four and six rayed star garnets. A six rayed star garnet exhibits needles aligned along the ⟨111⟩ and ⟨011⟩ directions of the garnet while a four rayed star garnet exhibits needles aligned along the ⟨111⟩ directions only. These results are believed to be applicable to asteriated garnets emanating from all sources. © *2006 Springer Science + Business Media, Inc.*

1. Introduction

The garnet group of minerals is very widespread and especially characteristic of metamorphic rocks of a wide variety of types, as well as being found in some granites and pegmatites, acid volcanic rocks and kimberlites. Moreover, they are often found in detrital sediments. The name 'garnet' derives from the Latin for grain because of the rounded crystals and similarity to the red blossoms of the pomegranate tree. As a group of minerals, garnets show one of the widest ranges of colors missing only the blue hue and for centuries the better quality almandines and pyropes were mistaken for rubies.

Some cut garnets are characterized by the presence of stars (asterism) and these stones, which are often prized, may be referred to as asterias. There are only a few known sources of asteriated garnets (Idaho, India, Sri Lanka, and Tanzania) [1]. Asteriated garnets from Emerald Creek, Latah County, Idaho, were the object of this study and they occur in hues of dark purple, light purple or dark red. Latah County is world famous as the source of almandine crystals that will produce asteriated gemstones. Because of its abundance and wide distribution throughout the state of Idaho, garnet is one of the principle gem minerals and has resulted in the star garnet being adopted as the state gemstone in 1967. The first attempt at commercial exploitation took place sometime in the 1930s when the Spokane Garnet Company was organized to mine the stones for abrasive purposes.

The garnet structure is cubic (Ia3d) and its habits can be dodecahedral, icositetrahedral (less common), and combinations of both. Although a natural garnet of pure end member composition is very rare, garnets are classified mineralogically on the basis of end member species of idealized composition. These include almandine $Fe_3Al_2(SiO_4)_3$, pyrope $Mg_3Al_2(SiO_4)_3$, spessartine $Mn_3Al_2(SiO_4)_3$ and grossular $Ca_3Al_2(SiO_4)_3$. Garnet crystals range in size from as small as a few millimeters to as much as several centimeters and often have a high level of internal strain making the cutting of the crystals a delicate task. They are usually found in isolated granular crystals often in the form of a near perfect rhombic dodecahedron, as shown in Fig. 1a. The rhombic dodecahedron is a convex polyhedron with twelve rhombic faces. The long diagonal of each face is exactly $\sqrt{2}$ times the length of the short diagonal, so that the acute angles on each face measure $2\tan^{-1}(1/\sqrt{2})$, or 70.53°.

Figs 1b and c show two fine examples of Idaho star garnets cut en cabochon, its base exactly parallel to the crystal face selected, with its apex in the center of the face. The white star pattern seems to glide or float across the darker surface of the stone as the viewing direction changes. If the cabochon is cut with a high crown, the star will stay on top of the stone when it is tilted back and forth. The shallower the cabochon, the more mobile the star becomes and the more rapidly it will move across the face of the stone. The value in relation to their size depends

0022-2461 © *2006 Springer Science + Business Media, Inc.*
DOI: 10.1007/s10853-006-6500-4

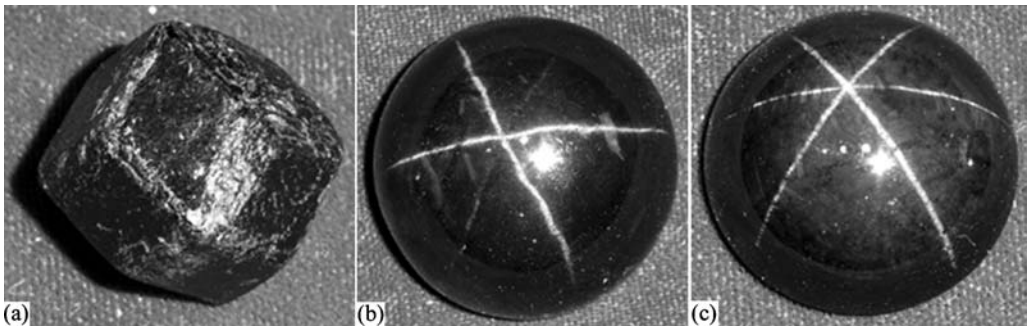

Figure 1 (a) Garnet crystal (9 carats) exhibiting the rhombic dodecahedral habit. Asteriated garnets cut *en cabochon* revealing, (b) a four-rayed and (c) a six-rayed star, weighting 110 and 46 carats, respectively.

entirely upon the brightness of the star, the number of rays (normally four, but occasionally six as in sapphire), and its proper orientation with the rays ideally intersecting exactly at the apex of the cabochon.

Much consideration has been given to the reasons for the production of the star like effect [1–7]. Garnets are indeed hosts to an interesting variety of inclusions, which reflect their somewhat diverse geological environments. It is the general belief that asterias result from submicron acicular inclusions of rutile, which we have now clearly proven to be the case. The needles result in the silky appearance of the interior of the stones, and these inclusions are sometimes referred to as "silk" [4]. Asterism can be considered as multiple chatoyance brought about by the scattering of light at right angles to the direction of the needles. If only one set of needles are present, as occasionally may happen, the scattering will then be limited to only one set of scattering cones, and only one ray of light will then be seen in a suitably cut stone. Under these conditions a "cat's eye" will be produced. The asterism is at its best advantage for stones that are cut and polished in the cabochon style and illuminated by a source of parallel light, e.g., the sun. What makes asteriated garnets special is the fact that stones may show either a four rayed star or both the four and six rayed stars, and crystals cut as complete spheres may show multiple asterism.

None of the previous studies on asterism in garnets have used Idaho garnets and none have confirmed the origin of the asterism using transmission electron microscopy (TEM). Schmetzer [1] used electron probe microanalysis (EPMA) and Raman spectroscopy to identify rutile needles in star garnets from Madagascar and the origin of the asterism was discussed in relation to the habit of the garnet crystal and the way it is cut [2, 3]. Exsolved titanium bearing phases are common in garnets and Zhang *et al*. [8] have explained the occurrence and characteristics of porphyroblastic garnet containing exsolved rutile needles. Ti solubility was found to be positively correlated with pressure. During isothermal decompression, rutile exsolves from the garnet along crystallographically controlled planes, giving rise to a star pattern on properly cut stones.

Star sapphires have drawn a little more attention and several detailed microscopy studies have been published [9–12]. Phillips and coworkers [12] confirmed using TEM that asterism in star sapphire was due to rutile (r) needles. This supported the much earlier suggestion for the origin of asterism in star sapphire [13]. The needles lie parallel to the three $\langle 10\bar{1}0\rangle$ directions and have the following relationship with the sapphire (s) matrix: $\langle 01\bar{1}\rangle_r // \langle 10\bar{1}0\rangle_s$ and$\{011\}_r // \{1\bar{2}10\}_s$. Moon and Phillips [9] identified both rutile precipitates and orthorhombic α-TiO_2 precipitates in natural blue sapphire but did not relate these precipitates to asterism.

It is interesting to point out that garnets are also high-technology materials of current research activities and not only attractive gemstones. Garnets are important crystals for solid-state lasers [e.g., 14] as well as for phosphor applications [15]. Also, Ce-doped YAG (Ce: $Y_3Al_5O_{12}$) is a promising material for X-ray imaging especially in various digital detectors [16]. New garnet films for magneto-optical photonic applications have been synthesized [e.g., 17].

The aim of this present study is to determine conclusively the origin of asterism in star garnets and the microstructural factors affecting their quality.

2. Experimental details

Four asteriated garnets from Emerald Creek, Latah County, Idaho were used in this study. All stones displayed a weak asterism that prescribed them from being classified as good quality gemstones. Asteria 1 displayed a four rayed star. Asterias 2 and 3 displayed six rayed stars while asteria 4 displayed both four and six rayed stars. EPMA was used to determine the average chemical compositions of the four asterias. A Cameca Camebax instrument operated with a 12 nA/20 kV electron beam was used to probe thin sections of the stones, polished to 1 μm using diamond compounds. The compositions were obtained by averaging several measured concentrations. Thin sections from the garnet crystals were polished and examined with an optical microscope. Numerous samples were prepared from these asterias using conventional

techniques (grinding, polishing, and dimpling) for TEM analysis. Perforation was obtained by ion milling (South Bay Technology XLA 2000) with 6 kV argon ions and a current of ~2 mA. TEM sample preparation is a challenge for naturally occurring minerals like garnets. They are brittle and inclusions may cause the stones to shatter while cutting or grinding because of the associated high internal strains. The electron transparent region in a TEM sample is so small that it is unlikely that it contains a good quality rutile crystal, either lying parallel to the thin foil or cross-sectioned perpendicular to its length. A thin film of carbon (<5 nm) was sputtered on the samples to avoid charging under the electron beam. Samples were examined using a Philips CM-200 TEM operated at 200 kV. High-resolution transmission electron microscopy was performed using a JEOL 2010 HRTEM operated at 200 kV.

3. Results

The chemical compositions of the four asterias are listed in Table I, yielding an average chemical formula $(Fe_{2.455}Mg_{0.495}Mn_{0.080}Ca_{0.042})Al_2(SiO_4)_3$. No distinct chemical zoning was observed. Almandine and pyrope being the two most abundant end members, the garnets are therefore referred to as almandine-pyropes (pyralspite series).

Natural garnets invariably contain inclusions. Microscopic examination revealed a singular kind of interior with an inclusion system of closely spaced, very fine, acicular crystals, with a definite angular relationship. Examination of cut cross sections of most garnet crystals revealed that the acicular crystals are not evenly distributed throughout the host crystal but instead lie in layers as shown in Fig. 2a, for a four rayed star stone. The needles, which are usually in two directions, intersect to form angles of approximately 70° and 110° (inset in Fig. 2b). Numerous large crystals, in the form of flakes of hundreds of micrometers across, were present throughout the garnets studied. The chemical composition of these flakes was shown by EPMA to be that of ilmenite ($FeTiO_3$). Also, some small zircon ($ZrSiO_4$) crystals on the order of micrometers were found to be present in the garnet matrix.

TABLE I Composition of the studied almandine-pyrope asterias from Emerald Creek, Idaho, determined by electron microprobe analysis

Asteria	1	2	3	4
Oxides (Wt.%)				
FeO	34.38	38.24	36.95	37.39
MgO	4.37	4.17	3.93	4.15
MnO	2.49	0.33	1.66	0.28
Al_2O_3	21.33	21.73	21.42	21.34
SiO_2	36.75	36.96	36.95	36.84
CaO	0.78	0.40	0.459	0.31
TiO_2	0.02	0.03	0.05	0.01
Cations based on 12 oxygens				
Fe	2.309	2.536	2.464	2.511
Mg	0.523	0.493	0.467	0.497
Mn	0.169	0.022	0.112	0.019
Al	2.019	2.031	2.013	2.019
Si	2.951	2.931	2.946	2.958
Ca	0.067	0.034	0.039	0.027
Ti	0.001	0.002	0.003	0
Mole % end-members				
Almandine	75.26	82.20	79.95	82.22
Pyrope	17.04	15.98	15.15	16.27
Spessartine	5.51	0.71	3.63	0.62
Grossular	2.18	1.10	1.12	0.88

Chemical microanalysis of single needles could neither be performed using energy dispersive X-ray microanalysis in the TEM nor with the electron microprobe because they were too small. This always resulted in an overlap of the chemical compositions of the garnet and the needles due to the X-ray excitation volume being larger that the needles themselves, leading to inconclusive results. However, X-ray mapping of the element titanium using the microprobe in a region containing a needle confirmed

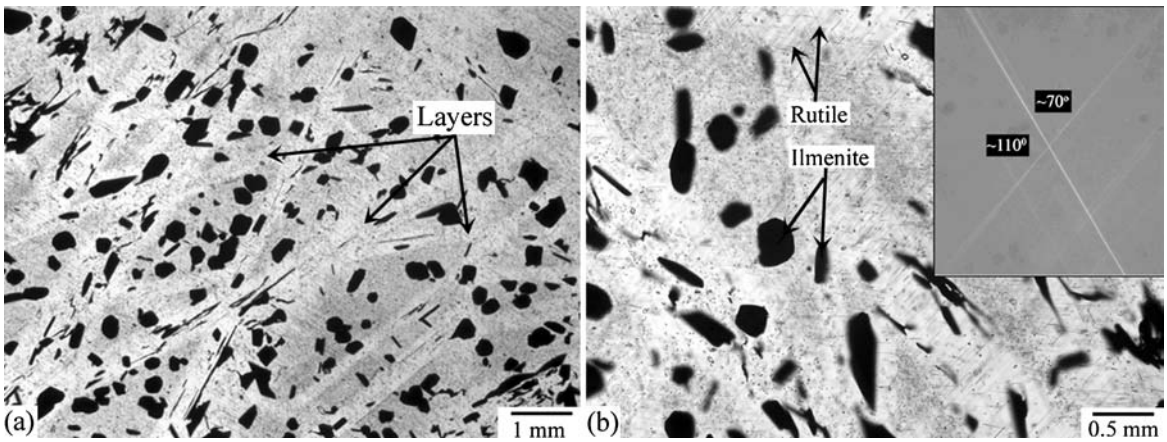

Figure 2 Optical micrographs of a cross section from a four rayed star garnet. (a) The rutile needles lie in layers and are not evenly distributed throughout the garnet host crystal. (b) Large ilmenite crystals with no preferred orientation are present in this sample. The insert is a reflected light micrograph showing two acicular inclusions of rutile intersecting each other at specific angles.

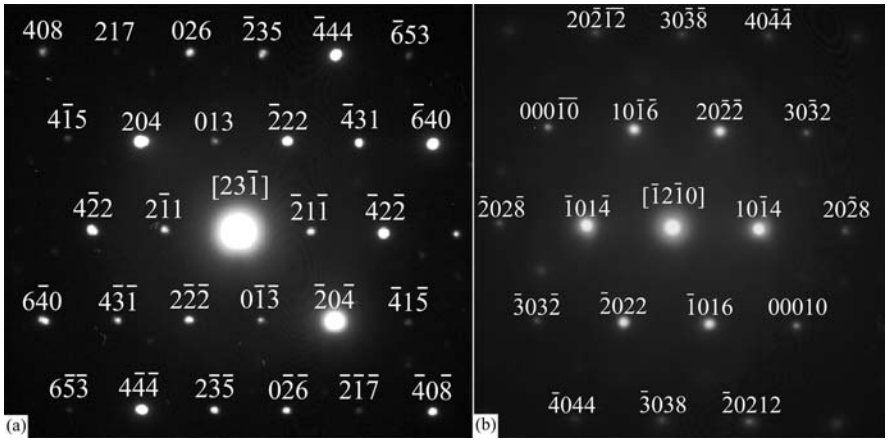

Figure 3 (a) DP of the garnet matrix at the $[23\bar{1}]$ zone axis. (b) DP of an ilmenite inclusion at the $[\bar{1}2\bar{1}0]$ zone axis.

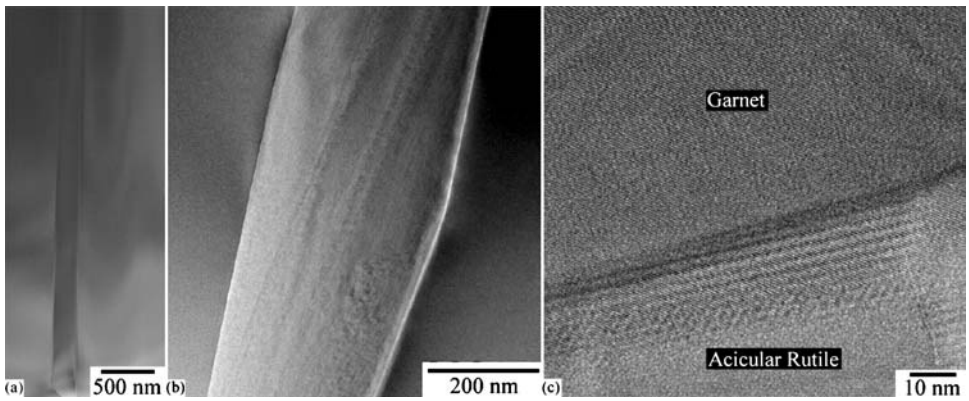

Figure 4 (a) TEM and (b) HRTEM images of rutile needles embedded in their host garnet. (c) HRTEM image of the interface between the garnet matrix and an acicular crystal of rutile.

that they do contain Ti, while the garnet matrix was found to be free of Ti, as expected.

Electron diffraction confirmed the structure of the garnet matrix. Fig. 3a shows an electron diffraction pattern obtained at the garnet $[23\bar{1}]$ zone axis. The large inclusions were confirmed from electron diffraction patterns to be ilmenite ($R\bar{3}$) and an indexed pattern at the$[\bar{1}2\bar{1}0]$ zone axis is shown in Fig. 3b. Electron microscopy showed the needles to have diameters predominantly on the order of 200 nm as illustrated in Fig. 4a, with lengths of hundreds of micrometers. Occasionally much wider needles were found, as shown in Fig. 4b. A HRTEM image of a garnet/needle interface is shown in Fig. 4c. The interfaces are fairly smooth and regular with no apparent cracks. The presence of moiré fringes in the images close to the needle/matrix interface suggests that the needle is inclined to the electron beam. Electron diffraction patterns obtained from the needles could be indexed to rutile, the stable phase of TiO_2. Fig. 5a shows a diffraction pattern that was obtained with both a rutile needle and the garnet host oriented on low index zone axes. This diffraction pattern was indexed to garnet at the [011] zone axis and to rutile at the $[0\bar{1}1]$ zone axis. For ease of comprehension, schematics of the diffraction patterns at the same scale are shown in Figs 5b–d.

The small diameter of the needles made indexing of electron diffraction patterns more difficult due to the presence of extra reflections from both phases and from double diffraction. The most informative experiments were performed using end-on needles, as it was possible to get both the needle and the garnet matrix on low index zone axes. It was therefore not possible to fully characterize a large quantity of these needles, in all possible directions.

Fig. 6a is a bright field image of a rutile needle oriented perpendicular to the specimen surface, a very rare occurrence. The rutile crystal exhibits sharp interfaces with the garnet host and moiré fringes are clearly visible in the image around the rutile needle where it is inclined to the surface plane. The average separation between the fringes is 2.6 nm. A diffraction pattern recorded at this orientation is shown in Fig. 6b.

4. Discussion

The general belief has been that the origin of asterism in star garnets is due to the presence of ru-

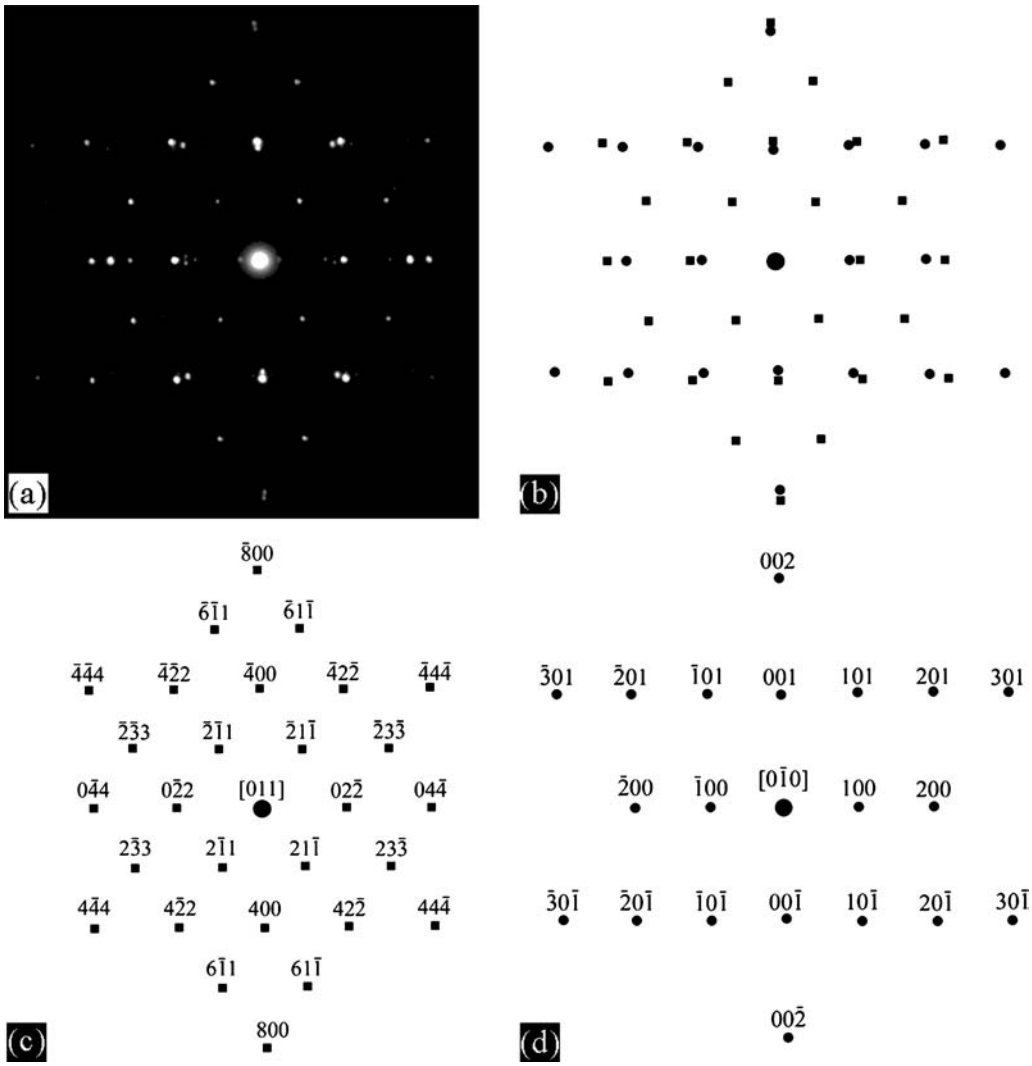

Figure 5 (a) Electron diffraction pattern of the garnet matrix and a rutile needle at the [011] and $[0\bar{1}0]$ zone axis, respectively. (b) Schematic of the diffraction pattern shown in (a). Filled squares and circles represent reflections from the garnet and rutile phases, respectively. (c) Schematic diffraction pattern giving indices of reflections for the garnet matrix at the [011] zone axis. (d) Schematic diffraction pattern giving indices of reflections for the rutile inclusion at the $[0\bar{1}1]$ zone axis.

tile needles. However, unlike in the case of star sapphires this assertion has remained crystallographically unproved. The electron diffraction patterns obtained in this study demonstrate clearly that the needles are indeed rutile. Our results are in contradiction with the belief of Gubelin [4] that the needle- and rodlike minerals inclusions in almandines and pyropes are hornblende crystals ($Ca_2(Mg,Fe)_4AlSi_7AlO_{22}(OH)_2$) or chrysotile ($Mg_3(Si_2O_5)(OH)_4$). However, his analysis was solely based on the appearance of these inclusions. In addition to confirming the crystal structure of the needles the diffraction patterns allow the orientation relationships between specific rutile inclusions and the garnet matrix to be determined. In this particular case, the orientation relationship was found to be $(02\bar{2})_g // (100)_r$, $(\bar{4}00)_g // (001)_r$, and $[011]_g // [0\bar{1}0]_r$. The subscripts g and r refer to the garnet and rutile phases, respectively. For this specific needle, we can therefore conclude that it grows along its a-axis, [010], in the garnet matrix in the [011] direction.

The associated images of end-on needles exhibit moiré fringes resulting from interference between diffracted beams from the rutile and garnet crystals and the direct beam. The moiré fringe spacing d_{tm} can be predicted in the absence of any rotation by Equation 1

$$d_{tm} = \frac{d_g}{\left(1 - \frac{d_g}{d_r}\right)} \tag{1}$$

where d_g and d_r are the interplanar spacings of the garnet and rutile, respectively. For $d_g = d_{(\bar{4}00)}$ and $d_r = d_{(\bar{1}\bar{1}0)}$, the predicted moiré fringe spacing is $d_{tm} = 2.5$ nm, which is very close to the measured value. The presence of moiré fringes indicates that the interface between the rutile and garnet cannot be coherent. If the interface is crystalline

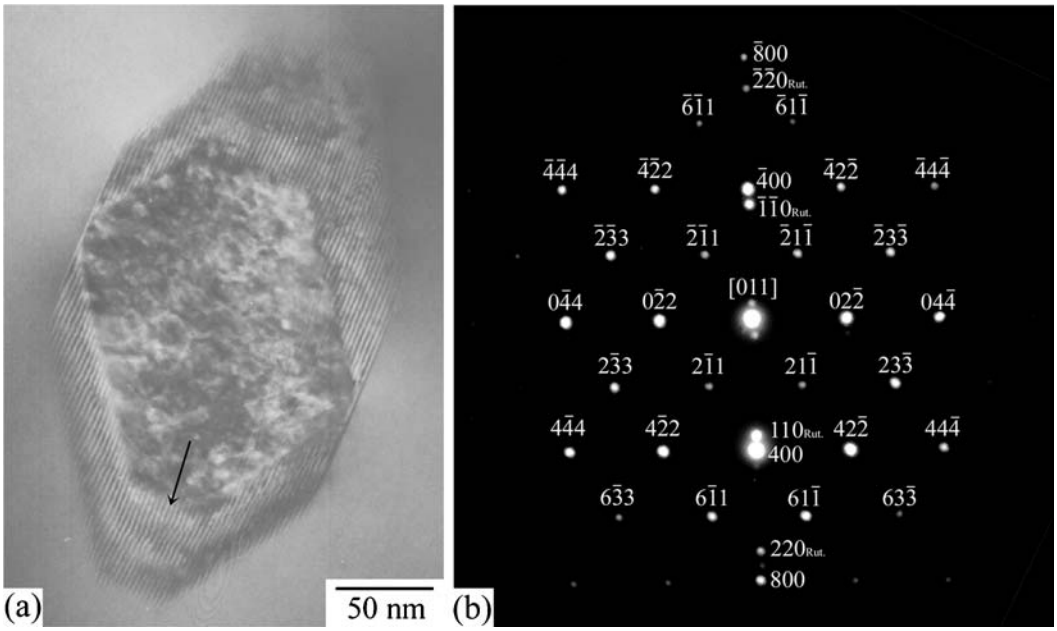

Figure 6 (a) BF image of a rutile needle pointing out of the TEM foil displaying two sharp interface with its garnet host. The arrow shows a dislocation formed to reduce the interfacial strain due to the lattice mismatch between the rutile and the garnet. (b) The electron diffraction pattern of the garnet matrix at the [011] zone axis with additional reflections due to the rutile needle.

and not simply incommensurate, then part of the interfacial strain must have been relieved by the formation of misfit dislocations. Moiré patterns can be used to locate and give information on dislocations which are present, the image then appearing as a magnified view of the projection of the dislocation. The terminating fringe, indicated by an arrow in Fig. 6a, shows the location of an interfacial dislocation that has been introduced to alleviate the lattice strain due to the garnet/rutile mismatch.

Using the lattice parameters of rutile ($a = b =$ 0.459 nm, $c = 0.296$ nm) and almandine garnet (a~1.15 nm), the lattice mismatches can be calculated. For rutile needles growing along the ⟨011⟩ directions, the mismatch between the $(02\bar{2})_g$ and $(100)_r$ planes is 12% while the mismatch between the $(\bar{4}00)_g$ and $(001)_r$ planes is 3%. The high degree of orientation of the needles is remarkable considering the quite large lattice mismatch. The morphology and crystallographic orientation of the rutile needles are controlled by the constrained growth in the garnet matrix.

Optical microscopy of cross sections from asteriated garnets show the acicular crystals of rutile to have their elongated directions separated by angles of ~70° and ~110°, which is in agreement with Wallcott who measured 70°32′ and 109°28′ [2]. We may therefore consider a portion of the rutile crystals to grow along the ⟨011⟩ directions of the garnet matrix, as we have deduced from the electron diffraction patterns; i.e., parallel to the edges of the octahedron. An observation consistent with that of Schmetzer [1]. Based on this assumption and by carefully examining a star pattern of the type shown in Fig. 1c, for a six rayed star garnet cut en cabochon, we can deduce the crystallographic orientation relationships between sets of rutile needles.

An important concept in the formation of asterism is that it is due to scattering of the incident light by multiple sets of rutile needles at right angles to the needle direction. Therefore, a four rayed star garnet will show two bands of scattered light separated by angles of ~70° and ~110°, which is consistent with the cubic symmetry of the garnet crystal (the angles between ⟨111⟩ directions are exactly 70.53° or 109.47°). Note that these angles are also consistent with the habit of the garnet crystals (i.e., rhombic dodecahedron) since the acute angles on each face are also equal to 70.53°.

For a six rayed star garnet there is an additional band of scattered light, which is located exactly in the middle of the obtuse angle formed by the two sets of needles lying in the ⟨111⟩ directions. In other words, the third band appears ~55° away from the ⟨111⟩ directions. This band of light corresponds to needles that are perpendicular to this direction, that is they lie at ~35° from the ⟨111⟩ direction, i.e., in the ⟨011⟩ directions.

These angular relationships are summarized in Fig. 7 and the following conclusions can be made: Four rayed asterism is produced when only two sets of rutile needles are visible and oriented along the ⟨111⟩ directions of the garnet matrix. A stone showing both four and six rayed asterism exhibits an additional set of rutile needles oriented along the ⟨011⟩ direction of the garnet matrix. This interpretation is consistent with the appearance of the star pattern on the surface of properly cut garnets. We

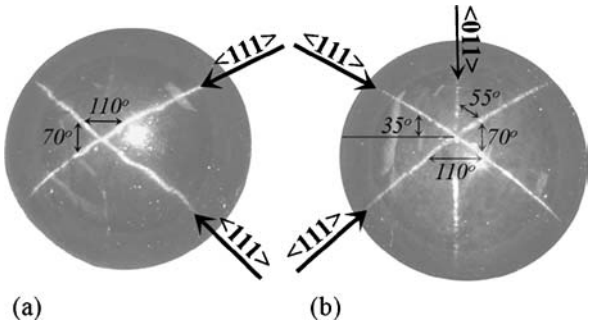

Figure 7 Montage showing a four rayed (a) and a six rayed (b) star garnet cut en cabochon. Superimposed to these photographs are the angular relationships with respect to the directions of the rutile needles inside the garnet matrix. Note that the light is scattered at right angles to the direction of the needles.

can also deduce that a "cat's eye" will be produced if only one set of needles, oriented along a ⟨011⟩ direction, is visible. Because the ⟨011⟩ and ⟨111⟩ directions are not parallel it is not possible to observe all three sets of rutile needles aligned along these directions at the same time from a cross section of a star garnet, but only the two sets of needles aligned along the ⟨111⟩ directions. Therefore, asteriated garnets cut as complete spheres show an interesting pattern consisting of multiple four and six rayed stars [1, 3].

For high quality asterism, it is necessary that the cross section of the rutile needles is of the order of the wavelength of the visible light (in the range 420 nm to 700 nm). In star sapphires rutile needles having lengths ranging up to some hundreds of microns with widths of ∼500 nm have been found [12]. However, the rutile crystals in the stones studied here had diameters of only about 200 nm in most cases. Also, we noted that the asterias were hosts to numerous large inclusions of ilmenite, which did not show any preferred orientation. Asterias containing the most ilmenite inclusions tended to yield a weaker asterism because the light scattered from the rutile needles may be attenuated by absorption, refraction and diffraction. The combination of these two factors—needle size and the presence of impurities—may be the cause of weak asterism in the garnets studied. The rutile needles in sapphires lie parallel to the faces of the hexagonal prism and in planes perpendicular to the c-axis forming a hexagonal pattern when viewed along the direction of this main crystal axis. On the other hand, in garnets the arrangement of the needles is more sporadic (and in the form of layers) and may be the reason why good quality garnet asterias are not as likely as sapphire asterias. The maximum brightness of a star would be displayed when the face of the cabochon is in a rutile-containing layer. Therefore, weak stars may be strengthened by deeper grinding. Conversely, a bright star may be weakened by deeper grinding, the face passing from being in a layer of rutile to a layer free of rutile.

5. Conclusion

We have conclusively identified the acicular crystals responsible for the asterism in star garnets as rutile, the stable phase of TiO_2. The crystallographic relationship of one set of rutile needles with respect to its garnet host has been determined to be $[011]_g // [0\bar{1}0]_r$, $(02\bar{2})_g // (100)_r$, $(\bar{4}00)_g // (001)_r$. Four rayed star garnets are the result of two sets of rutile needles aligned along the ⟨111⟩ directions of the garnet matrix being visible, while six rayed star garnets exhibit an additional set of rutile needles oriented along a ⟨011⟩ direction. Weak asterism results when the diameters of the rutile needles are less than the wavelength of light and when the stones contain large amounts of impurities.

Acknowledgments

The authors are grateful to Bill and Diane Mabbutt, owners of Gem State Crystals, Inc., Moscow, ID for kindly providing the garnets and to David Bahr for helpful discussions. Also, we wish to thank the EMSL, a national scientific user facility sponsored by the DOE, located at Pacific Northwest National Laboratory, where HRTEM images were collected.

References

1. K. SCHMETZER, H.-J. BERNHARDT and L. KIEFERT, *J. Gemm.* **28** (2002) 13.
2. A. J. WALLCOTT, *Geological Series of Field Museum of Natural History* **7** (1937) 39.
3. W. L. D. R. A. KUMARATILAKE, *J. Gemm.* **26** (1998) 24.
4. E. J. GUBELIN, in "Inclusions as a Means of Gemstone Identification" (Gemological Institute of America, 1953) p. 166.
5. R. WEBSTER, in "Gems", 3rd Edition (Butterworth and Co., 1975).
6. W. SCHUMANN, in "Gemstones of the World" (Sterling Publishing Co., New York, 1997).
7. K. LYMAN (Ed.), in "Gems and Precious Stones" (Simon and Schuster's Inc., New York, 1986).
8. R. Y. ZHANG, S. M. ZHAI, Y. W. FEI and J. G. LIOU, *Earth Planet. Sci. Lett.* **216** (2003) 591.
9. A. R. MOON and M. R. PHILLIPS, *Phys. Chem. Miner.* **18** (1991) 251.
10. D. S. PHILLIPS, B. J. PLETKA, T. E. MITCHELL and A. H. HEUER, *Proceedings of EMAG 75 held at the University of Bristol* (1975) 493.
11. S. Q. XIAO, D. A. PHILLIPS and A. H. HEUER, *Proceedings of the 51st Annual Meeting of the Microscopy Society of America* (1993) 954.
12. D. S. PHILLIPS, A. H. HEUER and T. E. MITCHELL, *Philos. Mag.* **A42** (1980) 385.
13. G. TSCHERMAK, *Mineralogische Mittheilungen* **1** (1878) 362.
14. D. E. EAKINS, M. HELD, M. G. NORTON and D. F. BAHR, *J. Cryst. Growth* **267** (2004) 502.
15. J.G. ZHOU, F.Y. ZHAO, Z.Q. LI, S.P. XIA, L. YANG and S.-Y. GAO, *J. Mater. Sci. Lett.* **39** (2004) 4711.
16. I. KANDARAKIS and D. CAVOURAS *et al.*, *Nucl. Instrum. Methods Phys. Res.* **A538** (2005) 615.
17. S. I. KHARTSEV and A. M. GRISHIN, *Appl. Phys. Lett.* **86** (2005) 1.